cation shows that it is closest to that theoretically predicted for a partially methyl-bridged structure.

Acknowledgment. S.A.J. thanks Drs. Bill Brennan, Hugh Munro, and Dick Hutton for many stimulating discussions and the SERC for provision of a research studentship. We thank Rob Allaker for preparing the norbornyl chloride and Dr. Gerald Brooke for providing the butene.

Registry No. Antimony pentafluoride, 7783-70-2; *tert*-butyl chloride, 507-20-0; *exo*-2-norbornyl chloride, 765-91-3; 2-norbornene, 498-66-8; fluorosulfonic acid, 7789-21-1; *cis*-but-2-ene, 590-18-1; *tert*-butyl cation, 14804-25-2; 2-norbornyl cation, 24321-81-1; *sec*-butyl cation, 16548-59-7.

σ/π Interactions in [2.2]Paracyclophanes. PE Investigations on Octamethyltetrasila[2.2]paracyclophane and Octamethyltetrasila[2.2](2,5)thiophenophane and -furanophane

Rolf Gleiter,*,† Wolfgang Schäfer,† Gerhard Krennrich,† and Hideki Sakurai*,‡

Contribution from the Institut für Organische Chemie, Universität Heidelberg, D-6900 Heidelberg, West Germany, and Department of Chemistry, Tohoku University, Sendai 980, Japan. *Received November 13, 1987*

Abstract: The photoelectron spectra of 1,1,2,2,9,9,10,10-octamethyl-1,2,9,10-tetrasila[2.2]paracyclophane (**6a**) and the related octamethyltetrasila[2.2](2,5)thiophenophane (**7a**) and -furanophane (**8a**) have been recorded. The sequence of the first bands of these spectra is assigned by comparison of the ionization energies with calculated orbital energies. A comparison between the band sequence of **6a** and that of [2.2]paracyclophane (**1**) shows a smaller through-space and a larger through-bond interaction for **6a**. The through-bond interaction between the $b_{3u}(\sigma)$ orbital and the corresponding π orbital yields a different orbital sequence in **6a** as compared to **1**. A similar strong through-bond interaction as in **6a** has been encountered in **7a** and **8a** as shown by comparing the PE spectra of the latter compounds with [2.2](2,5)thiophenophane (**10**) and [2.2](2,5)furanophane (**11**).

The He I photoelectron (PE) spectrum of [2.2]paracyclophane (**1**) shows a broad first band between 8.0 and 8.4 eV, well separated from two smaller bands at 9.65 and 10.3 eV.[1] It is generally accepted that the first feature is due to the three different ionic states $^2B_{2g}$, $^2B_{3g}$, and $^2B_{3u}$ while the second band is assigned to $^2B_{2u}$.[1,2] A schematic drawing of the corresponding wave functions is given. A consideration of the wave functions corresponding to the four highest occupied MO's of **1** shows that the MO's that pertain to the irreducible representations b_{3g}, b_{2g}, and b_{2u} are pure π MO's, while b_{3u} has a considerable admixture of the C–C σ bonds connecting the two rings.[2,3] This difference in σ/π interaction can be used to investigate the sequence of the corresponding bands empirically. The σ/π mixing of the b_{3u} orbital can be increased or decreased by lowering or raising the energy of the $b_{3u}(\sigma)$ orbital, which interacts with $b_{3u}(\pi)$. An increase of $b_{3u}(\sigma)$ will increase σ/π mixing and thus will lower the orbital energy of b_{3u} and vice versa.


1

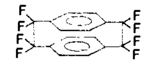
2

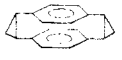
3

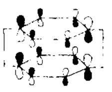
$b_{2g}(\pi_\perp^-)$

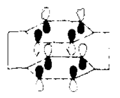
$b_{3g}(\pi_\parallel^-)$

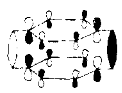
$b_{3u}(\pi_\perp^+)$

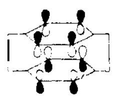
$b_{2u}(\pi_\parallel^+)$

Heilbronner and Maier[4] have studied a case where the σ/π interaction is lowered by investigation of 1,1,2,2,9,9,10,10-octafluoro[2.2]paracyclophane (**2**). Due to the inductive effect of the fluorine atoms, the ionization from the b_{3u} orbital of **2** occurs at considerably higher energy than from b_{2g} and b_{3g}. The opposite effect can be detected in the PE spectrum of [1,2:9,10]dimethano[2.2]paracyclophane (**3**).[5] In this compound the basis orbital energy of the σ bond of the three-membered rings in **3** is higher than the σ bonds in **1**, which leads to an increase of the σ/π interaction and thus lowers the energy associated to the ionization from the $b_{3u}(\pi)$ orbital. Due to the strong overlap of the first three PE transitions, the expected shift is, however, difficult to recognize.

Table I. Comparison between the Measured Ionization Energies, $I_{v,j}$, of **6a** and the Orbital Energies, ϵ_j, Calculated for **6b** Using the FMO Approach and the MNDO and the ab Initio Methods

band	$I_{v,j}$	assignment	$-\epsilon_j$(FMO)	$-\epsilon_j$(MNDO)	$-\epsilon_j$(STO-3G)
1	7.8	$6b_{3u}$	7.84	8.46	6.27
2	8.3	$5b_{2g}$	8.20	8.76	6.33
		$5b_{3g}$	8.40	8.98	7.10
3	9.2	$5b_{2u}$	9.40	9.83	7.11
4	9.8	$7a_g$	10.60	9.33	7.89

Recently,[6] we have shown that the replacement of a C–C σ bond in **4** by a Si–Si σ bond, **5**, has dramatic effects on the sequence of the highest occupied MO's. A comparison of the PE spectra

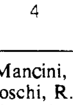
4

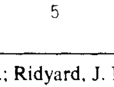

5

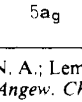
$5a_g$

---

[1] Pignataro, S.; Mancini, V.; Ridyard, J. N. A.; Lempka, H. J. *J. Chem. Soc. D* **1971**, *142*. Boschi, R.; Schmidt, W. *Angew. Chem.* **1973**, *85*, 408; *Angew. Chem., Int. Ed. Engl.* **1973**, *12*, 402. Koenig, T.; Tuttle, M.; Wielesek, R. A. *Tetrahedron Lett.* **1974**, *29*, 2537. Koenig, T.; Wielesek, R.; Snell, W.; Balle, T. *J. Am. Chem. Soc.* **1975**, *97*, 3225.

[2] Heilbronner, E.; Yang, Z. *Top. Curr. Chem.* **1983**, *115*, 1, and references therein.

[3] Gleiter, R. *Tetrahedron Lett.* **1969**, 4453.

[4] Heilbronner, E.; Maier, J. P. *Helv. Chim. Acta* **1974**, *57*, 151.

[5] Gleiter, R.; Eckert-Maksić, M.; Schäfer, W.; Truesdale, E. A. *Chem. Ber.* **1982**, *115*, 2009.

[6] Gleiter, R.; Schäfer, W.; Sakurai, H. *J. Am. Chem. Soc.* **1985**, *107*, 3046.

† Universität Heidelberg.
‡ Tohoku University.

0002-7863/88/1510-4117$01.50/0

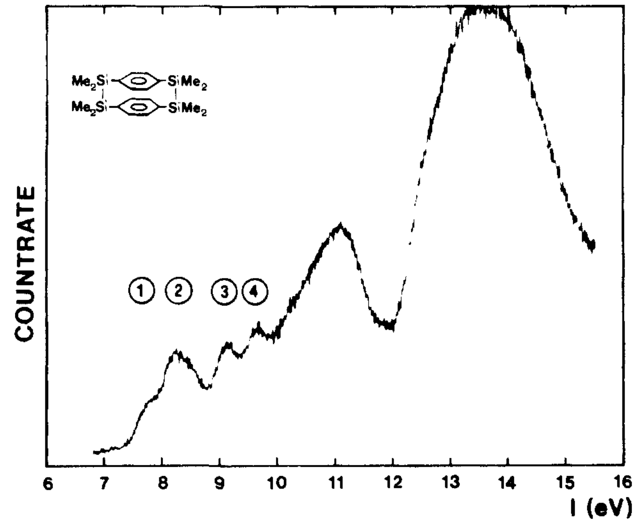

Figure 1. PE spectrum of **6a**.

of **4** and **5** shows a strong shift of the PE band assigned to ^2A_g of **4** (9.8 eV) compared to that in **5** (8.13 eV). These studies led us to predict[6] that, in a [2.2]paracyclophane bridged by two Si_2Me_4 units, similar effects are expected. The subsequent preparation of **6a**–**8a**[7,8] allows us to investigate the effect of such a bridge.

PE Spectrum and Orbital Sequence of 6a. In Figure 1 the PE spectrum of **6a** is shown. Its first bands are markedly different from those of **1**.[1,2] In the PE spectrum of **6a** a shoulder at 7.8 eV can be observed followed by a broad feature centered at 8.3 eV whereas the PE spectrum of **1** shows only one broad feature at 8.1 eV with a steep onset at the lower energy side. If one transition is assigned to the shoulder at 7.8 eV and the peak 3 at 9.2 eV, respectively, it seems reasonable to assign two transitions to the broad feature at 8.3 eV. The recorded vertical ionization energies, $I_{v,j}$, for **6a** are listed in Table I. To assign the bands in the recorded PE spectra to individual transitions, we rely on the validity of Koopmans' theorem ($I_{v,j} = -\epsilon_j$),[9] which allows one to relate the ionization energies, $I_{v,j}$, with the calculated orbital energies, ϵ_j. This approximation seems a reasonable one, at least for the first ionization energies of organic compounds.[9] To calculate the energies of the highest occupied molecular orbitals (MO's), the unsubstituted species, **6b**, was used as a model. The energies of the MO's are derived in two ways, either by empirically adopting a fragment molecular orbital (FMO) approach, as in the case of **5**,[6] or by using semiempirical and ab initio MO methods.

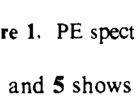
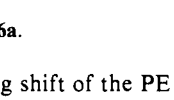
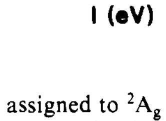

R=CH₃ **6a** **7a** **8a**

R=H **6b** **7b** **8b**

In the FMO approach, it is assumed that the first bands in the PE spectrum of **6a** are due to the ionization from π MO's that arise from the four linear combinations that can be constructed from the two highest occupied MO's of benzene ($\pi_\perp$ and $\pi_\parallel$).

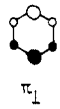

$\pi_\perp$

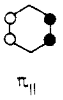

$\pi_\parallel$

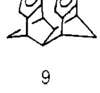

9

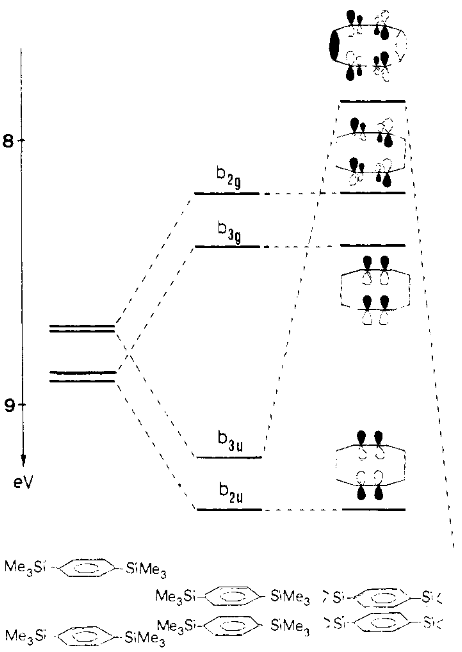

Figure 2. Through-space (middle) and through-bond (right) interaction between the four linear combinations b_{2g}, b_{3g}, b_{3u}, and b_{2u} arising from four π MO's of two *p*-bis(trimethylsilyl)benzene rings and **6a**, respectively.

These two MO's will give rise to four linear combinations, which are either bonding ($\pi_\perp^+$, $\pi_\parallel^+$) or antibonding ($\pi_\perp^-$, $\pi_\parallel^-$) with respect to the symmetry plane parallel to the benzene rings in **6a**. The four linear combinations belong to the irreducible representations B_{2g}, B_{3g}, B_{3u}, and B_{2u}, which are shown schematically in the previous section.

To set up the interaction matrix, the diagonal and nondiagonal elements have to be chosen. For the basis energy of the π MO's, we choose $\langle\pi|H|\pi\rangle$ to be -8.7 eV for $\pi_\perp$ and -8.9 eV for $\pi_\parallel$; these values are taken from the PE spectrum of 1,4-bis(trimethylsilyl)benzene.[11] For the basis energy of the Si–Si σ bond a value of -10.6 eV was chosen, in analogy to the diagonal element in **5**.[6] For the nondiagonal elements we choose for the interaction between the Si–Si σ bond and the π system a value of $\langle\pi|H|\sigma\rangle = -0.97$ eV. This value goes back to that chosen for **5**, corrected for the different AO coefficients of the acetylene as compared to the benzene ring. For the through-space interaction between the two benzene rings in **6a**, a value of $\langle\pi|H|\pi\rangle = -0.5$ eV was adopted. This value takes into consideration the fact that the separation between the center of both benzene rings in **6a** amounts to 3.4 Å.[7] A similar average distance is present in **9** for which the PE bands could be simulated by adopting a value of -0.5 eV for the through-space interaction.[12] With the diagonal and nondiagonal elements described, a 6 × 6 matrix can be set up. Its diagonalization yields the eigenvalues listed in Table I. Although this calculation has only qualitative character, it allows the estimation of the ratio of through-space and through-bond interactions in **6b** as well as the comparison with related species. Figure 2 shows an interaction diagram, which is based on the FMO model previously described. A relatively small through-space interaction is revealed, which is dominated by a strong through-bond interaction due to the relatively high orbital energy of the Si–Si σ bond.

Table I also lists the results of calculations using the MNDO method[13] and the restricted HF theory employing a STO-3G basis.[14] In the case of the MNDO calculations, the heat of

---

(7) Sakurai, H.; Hoshi, S.; Kamiya, A.; Hosomi, A.; Kabuto, C. *Chem. Lett.* **1986**, 1781.

(8) Sakurai, H.; Hoshi, S.; Sakamoto, K., submitted for publication in *Chem. Lett.*

(9) Koopmans, T. *Physica (Amsterdam)* **1934**, *1*, 104.

(10) Cederbaum, L. S.; Domcke, W.; Schirmer, J.; v. Niessen, W. *Phys. Scr.* **1980**, *21*, 481.

(11) We are grateful to I. Hargittai for providing us with a sample of 1,4-bis(trimethylsilyl)benzene.

(12) Prinzbach, H.; Sedelmeier, G.; Krüger, C.; Goddard, R.; Martin, H. D.; Gleiter, R. *Angew. Chem.* **1978**, *90*, 297; *Angew. Chem., Int. Ed. Engl.* **1978**, *17*, 271.

(13) Dewar, M. J. S.; Thiel, W. *J. Am. Chem. Soc.* **1977**, *99*, 4899.

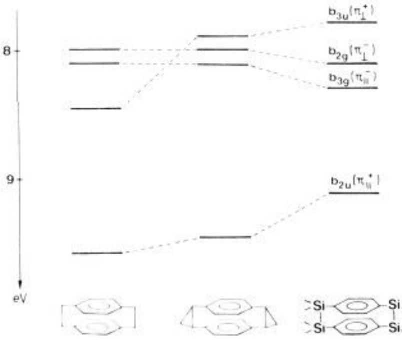

Figure 3. Correlation diagram between the first four bands of the PE spectra of **1**, **3**, and **6a**.

Table II. Comparison between the Measured Ionization Energies, $I_{v,j}$, of **7a** and **8a** with the Orbital Energies, ϵ_j, Calculated for **7b** and **8b** Using the HF ab Initio Approach with a STO-3G Basis and the MNDO Method

compd	band	$I_{v,j}$	assignment	$-\epsilon_j$(MNDO)	$-\epsilon_j$(STO-3G)
7a	1	7.4	$8a_u$	8.80	5.86
	2	8.0	$11a_g$	9.35	6.48
	3	8.4	$7b_g$	9.71	6.73
	4	8.7	$10b_u$	9.78	7.44
	5	9.4	$10a_g$	9.60	8.04
8a	1	7.4	$8a_u$	8.66	5.98
	2	8.1	$7b_g$	8.93	6.94
	3	8.9	$11a_g(\sigma)$	9.39	7.70
	4	9.4	$10b_u$	10.07	8.24
	5		$10a_g$	10.37	9.34

formation with respect to all geometrical variables of **6b** was minimized. In the case of the ab initio procedure only the Si–Si bond length of **6b** was minimized. This proceeding seems reasonable in view of the observation that the calculated value of the Si–Si bond length (STO-3G basis) is shorter than the experimental one by about 0.1 Å[14b] and that the deviation between experiment and calculation is considerably larger for the Si–Si bond length than for the C–C bond length.[14b] The atomic coordinates predicted for the benzene part are close to the X-ray data reported for **6a**. The length of the Si–Si σ bond for **6b** is predicted to be 2.24 Å (MNDO/1) and 2.29 Å (STO-3G). The Si–Si bond length determined for **6a** is 2.376 Å.[7] Both calculations confirm the orbital sequence as derived by the FMO treatment. Besides the four π MO's discussed above, all calculations predict a high-lying σ MO ($7a_g$) localized at the Si–Si σ bonds. We assign this tentatively to band 4 at 9.8 eV.

In Figure 3 the first peaks of the PE spectra of **1**, **3**, and **6a** are correlated. This correlation points to a smaller split between $b_{3g}(\pi_\parallel^-)$ and $b_{2u}(\pi_\parallel^+)$ for **6a** (0.7 eV) as compared to **1** (1.5 eV) and **3** (1.4 eV). This result seems reasonable in view of the larger distance between the benzene rings in **6a** (3.4 Å) compared to **1** (3.1 Å).

PE Spectra of 7a and 8a. The PE spectra of **7a** and **8a** are shown in Figure 4, and the measured vertical ionization energies are presented in Table II. To understand both spectra and to relate its bands to the sequence of the highest occupied MO's, the PE spectra of [2.2](2,5)thiophenophane (**10**)[15] and [2.2](2,5)furanophane (**11**)[15] will be considered first. The PE spectrum of **10** closely resembles that of **1** with respect to the first four transitions. Also, a broad feature around 8.2 eV is observed for which the transitions from $8a_u$, $11a_g$, and $7b_g$ can be assigned.[15] The second band has been ascribed to the ionization from $10b_u$.[15]

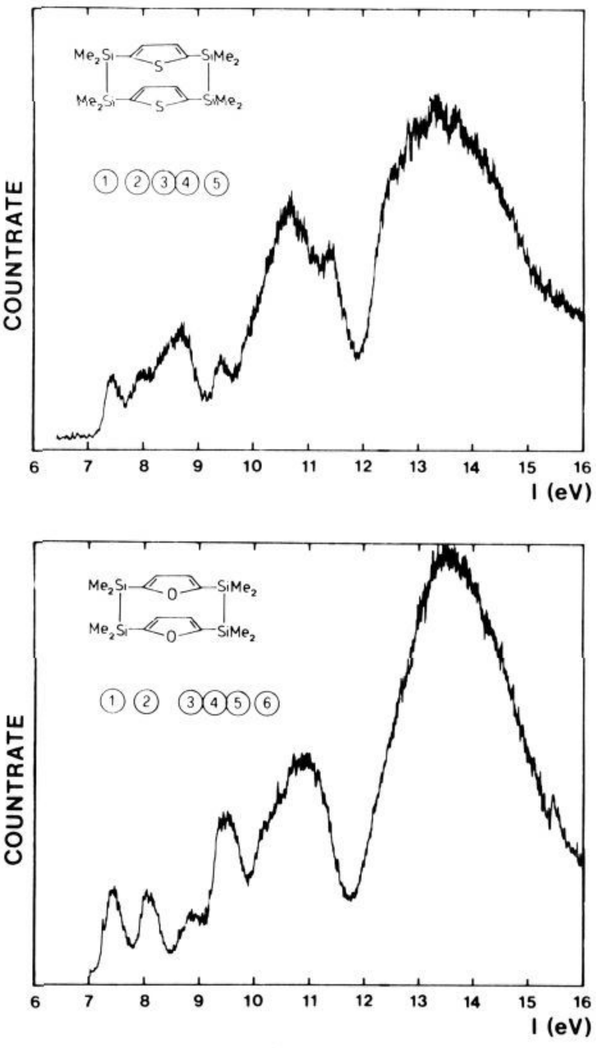

Figure 4. PE spectra of **7a** and **8a**.

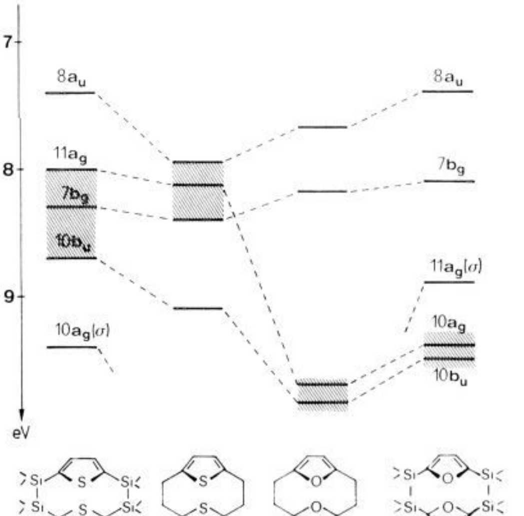

Figure 5. Correlation between the first four bands in the PE spectra of **7a** and **10** (left) and **8a** and **11** (right).

The PE spectrum of **11** shows two peaks at 7.6 and 8.2 eV, well separated from two close-lying transitions at 9.7 eV.

MO calculations on **10** and **11** suggest similar values for the orbital energies of $8a_u$ (HOMO) and $7b_g$ for both compounds but a large difference for $11a_g$ and $10b_u$. These results are depicted

---

[14] (a) Hehre, W. J.; Ditchfield, R.; Stewart, R. F.; Pople, J. A. *J. Chem. Phys.* **1970**, *52*, 2769. (b) Hehre, W. J.; Radom, L.; Schleyer, P. v. R.; Pople, J. A. *Ab Initio Molecular Orbital Theory*; Wiley: New York, 1986.

[15] Bernardi, F.; Bottoni, A.; Colonna, F. P.; Distefano, G.; Folli, U.; Vivarelli, P. Z. *Naturforsch., A: Phys., Phys. Chem., Kosmophys.* **1978**, *33a*, 959. Kovač, B.; Allan, M.; Heilbronner, E.; Maier, J. P.; Gleiter, R.; Haenel, M. W.; Keehn, P. M.; Reiss, J. A. *J. Electron Spectrosc. Relat. Phenom.* **1980**, *19*, 167.

in the middle of Figure 5 where the first four PE bands of **10** and **11** are correlated. Our correlation is based on ab initio calculations on **10** and **11** using a STO-3G basis adopting the geometrical parameters obtained from a X-ray study on **10** and **11**.[16] The wave functions that correspond to the four highest occupied MO's of **10** and **11** are shown schematically. The similarity with the

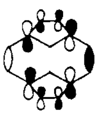
$a_u(\pi_{\parallel}^{+})$

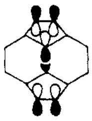
$a_g(\pi_{\perp}^{+})$

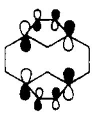
$b_g(\pi_{\parallel}^{-})$

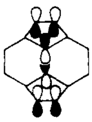
$b_u(\pi_{\perp}^{-})$

four highest occupied MO's of **1** is evident. The correlation shown in the center of Figure 5 follows also from the nodal properties of the wave functions. In $8a_u$ and $7b_g$ there is a node through the heteroatoms, while in $11a_g$ and $10b_u$ large coefficients at the heteroatoms are predicted. Thus, in the latter case the difference in electronegativity between S and O is mainly responsible for the strong stabilization of $11a_g$ and $10b_u$ in the case of **11** as compared to **10**.

The comparison of the orbital sequence of **1** with that in **6a** led us to anticipate two effects for the comparison of **7a** with **10** and of **8a** with **11**: (i) a strong destabilization of $8a_u$ due to the increased σ/π interaction when a C_2H_4 bridge is replaced by a $Si_2(CH_3)_4$ bridge and (ii) a smaller split between $10b_u$ and $11a_g$ in the case of the sila-bridged species (**7a**, **8a**) as compared to **10** or **11**, respectively, caused by the larger separation of the π systems in **7a** and **8a**. Figure 5 shows the correlation between the PE bands of **7a** and **8a** and those of **10** and **11** using the criteria outlined above. As in the case of **6a**, one encounters in the PE spectra of **7a** and **8a** a high-lying σ band, which we ascribe tentatively to the ionization from the symmetric linear combination of the two Si-Si σ bonds (a_g). The assignment given in Figure 5 for **7a** and **8a** is also confirmed by MO calculations using the restricted HF theory employing a STO-3G basis[14] (see Table II). For these calculations we adopted for **7a** and **8a** the anti conformation of both heterorings and the same geometrical parameters of the thiophene and furan moiety as present in **10** and **11**.[16] For the Si-Si bond length we choose a value of 2.24 Å.

Conclusions

Our PE investigations on **6a–8a** reveal in all three cases a very strong interaction between the π MO of b_{3u} (**6a**) and $8a_u$ (**7a**, **8a**) symmetry, respectively, and the corresponding MO's mainly localized at the Si-Si σ bonds. The comparison between **1**, **3**, and **6a** (Figure 3) shows that the σ/π interaction of a highly strained C-C σ bond, as present in the cyclopropane moieties of **3**, is comparable to the Si-Si σ bond of **6a**. The comparison of the first PE bands of **7a–10** and **8a–11** indicates the same sequence of the highest occupied MO's in all four compounds; the comparison **1–6a**, however, yields a reversal of the HOMO. This finding is of interest with respect to the ESR spectra of the corresponding radical cations and reactions in which the symmetry of the HOMO is a determining factor.

Experimental Section

The syntheses of **6a–8a** have been reported in the literature.[7,8] The He I photoelectron spectra of the analytically pure compounds were recorded on a Perkin-Elmer PS 18 spectrometer. The recording temperatures were as follows: **6a** and **7a**, 140 °C; **8a**, 90 °C. The spectra were calibrated with argon and xenon. An estimated accuracy of ±0.05 eV was achieved for the single bands and of ±0.1 eV for the shoulders.

Acknowledgment. Financial support is gratefully acknowledged by the Fonds der Chemischen Industrie and the BASF Aktiengesellschaft in Ludwigshafen. We thank A. Flatow for measuring the PE spectra.

Registry No. 6a, 109828-61-7; **6b**, 114184-43-9; **7a**, 114184-41-7; **7b**, 114197-84-1; **8a**, 114184-42-8; **8b**, 114184-44-0.

---

[16] Bresciani-Pahor, N.; Calligaris, M.; Rondaccio, L. *J. Chem. Soc., Perkin Trans. 2* **1978**, 42.

High Molecular Weight Boron Oxides in the Gas Phase

Robert J. Doyle, Jr.

Contribution from the Chemistry Division, Code 6112, Naval Research Laboratory, Washington, D.C. 20375-5000. *Received December 9, 1987*

Abstract: A new class of gas-phase boron oxides has been produced by particle-induced desorption from vitreous boron trioxide. Six distinct homologous series of boron oxide cations were identified by fast atom bombardment mass spectrometry and studied by collision-induced dissociation. Common structural features within each series were confirmed by the identification of common collision-induced fragments. Two important series are described by the general formulas $[B_{2n+1}O_{3n+1}]^+$ (n = 0–6) and $[B_{2n+2}O_{3n+3}]^{\bullet+}$ (n = 0–4). Ions of the first series show the highest relative abundances in the desorption spectrum of boron trioxide and are the most abundant ionic fragments in the collision spectra of nearly all boron oxide cations. The most important of these is $[B_3O_4]^+$, which is proposed to exist as $[O{=}B{-}O{-}B{-}O{-}B{=}O]^+$ and is stabilized by extensive resonance and electron sharing. Gas-phase boron oxide cations are proposed to exist with boron limited to two- or three-coordination with oxygen. The ions are thus built upon integral BO_3 triangles, and branches are terminated with $-B{=}O$ units.

Polymeric boron oxide anions, in the form of polyborate ions, are well-known components of crystalline borate salts.[1] Although simple boron–oxygen cations and anions such as BO^+, $B_2O_3^{\bullet+}$, and BO_2^- have been isolated in the gas phase, there has been no evidence for the existence of polymeric boron–oxygen species in the gas phase. The difficulty of predicting the existence of such species arises from structural uncertainties because of the interchangeability of boron coordination.

Boron–oxygen compounds are observed typically with boron assuming a three- or fourfold coordination with oxygen. The most common oxidation state of boron (+3) is the result of sp^2 hybridization that is responsible for the formation of three triangular-planar bonds with oxygen. The low-energy fourth orbital of the boron valence shell is responsible for its Lewis acid prop-

---

[1] Muetterties, E. L. *The Chemistry of Boron and Its Compounds*; Wiley: New York, 1967; pp 166–176.

[2] White, D.; Walsh, P. N.; Mann, D. E. *J. Chem. Phys.* **1958**, *28*, 508–509. White, D.; Mann, D. E.; Walsh, P. N.; Sommer, A. *J. Chem. Phys.* **1960**, *32*, 481–487.